RESEARCH PAPER

BJP BRITISH PHARMACOLOGICAL SOCIETY

Cytokine activin C ameliorates chronic neuropathic pain in peripheral nerve injury rodents by modulating the TRPV1 channel

Ya-Kun Huang[1,2] | Yu-Gang Lu[3] | Xin Zhao[4] | Jing-Bing Zhang[2] |
Feng-Ming Zhang[1] | Yong Chen[1] | Ling-Bo Bi[1] | Jia-Hui Gu[1] | Zuo-Jie Jiang[2] |
Xiao-Man Wu[2] | Qing-Yi Li[2] | Yanli Liu[5] | Jian-Xin Shen[2] | Xing-Jun Liu[1,2] (ORCID)

[1]School of Pharmacy, Nantong University, Nantong, China

[2]Pain and Related Diseases Research Laboratory, Shantou University Medical College, Shantou, China

[3]Department of Anesthesiology, Shanghai Pulmonary Hospital, Tongji University School of Medicine, Shanghai, China

[4]Department of Geriatrics, Renji Hospital, School of Medicine, Shanghai Jiaotong University, Shanghai, China

[5]College of Pharmaceutical Science, Soochow University, Suzhou, China

Correspondence
Xing-Jun Liu, School of Pharmacy, Nantong University, R609, Building 3, 19 Qixiu Road, Nantong, Jiangsu Province 226001, China.
Email: edvin201@163.com

Background and Purpose: The cytokine activin C is mainly expressed in small-diameter dorsal root ganglion (DRG) neurons and suppresses inflammatory pain. However, the effects of activin C in neuropathic pain remain elusive.

Experimental Approach: Male rats and wild-type and TRPV1 knockout mice with peripheral nerve injury - sciatic nerve axotomy and spinal nerve ligation in rats; chronic constriction injury (CCI) in mice – provided models of chronic neuropathic pain. Ipsilateral lumbar (L)4–5 DRGs were assayed for activin C expression. Chronic neuropathic pain animals were treated with intrathecal or locally pre-administered activin C or the vehicle. Nociceptive behaviours and pain-related markers in L4–5 DRGs and spinal cord were evaluated. TRPV1 channel modulation by activin C was measured.

Key Results: Following peripheral nerve injury, expression of activin βC subunit mRNA and activin C protein was markedly up-regulated in L4–5 DRGs of animals **with axotomy, SNL or CCI.** [Correction added on 26 November 2020, after first online publication: The preceding sentence has been corrected in this current version.] Intrathecal activin C dose-dependently inhibited neuropathic pain in spinal nerve ligated rats. Local pre-administration of activin C decreased neuropathic pain, macrophage infiltration into ipsilateral L4–5 DRGs and microglial reaction in L4–5 spinal cords of mice with CCI. In rat DRG neurons, activin C enhanced capsaicin-induced TRPV1 currents. Pre-treatment with activin C reduced capsaicin-evoked acute hyperalgesia and normalized capsaicin-evoked persistent hypothermia in mice. Finally, the analgesic effect of activin C was abolished in TRPV1 knockout mice with CCI.

Conclusion and Implications: Activin C inhibits neuropathic pain by modulating TRPV1 channels, revealing potential analgesic applications in chronic neuropathic pain therapy.

5642 | wileyonlinelibrary.com/journal/bph Br J Pharmacol. 2020;177:5642–5657.

1 | INTRODUCTION

Chronic neuropathic pain, which affects a significant proportion of the general population and has substantial negative effects on patients, is caused by somatosensory nervous system lesions or specific disorders. Currently, mechanisms underlying neuropathic pain remain unclear (Huang et al., 2019; Ji, 2018; Kuner, 2010; Sun et al., 2017), and typically, patients with neuropathic pain are poorly served by existing therapies. Thus, it is imperative to explore novel therapeutic drugs or targets to improve therapeutic effectiveness (Obara, Telezhkin, Alrashdi, & Chazot, 2020; Percie du Sert & Rice, 2014). Accumulating evidence suggests that cytokine signalling plays a critical role in chronic neuropathic pain processing, and targeting these signalling pathways can reduce neuropathic pain in animal models (Agarwal et al., 2018; Baral, Udit, & Chiu, 2019; de Vries & MaassenVanDenBrink, 2019; Hung, Lim, & Doshi, 2017; Lees et al., 2015). Among these, the **TGF-β** superfamily was identified as a specific member, with ligands, signalling effectors, and modulators may be potential targets for novel therapeutic agents in neuropathic pain management (Dong & He, 2014; Lantero, Tramullas, Diaz, & Hurle, 2012). Preclinical and clinical data have revealed that the TGF-β family, the **activin and inhibin family**, the **bone morphogenetic protein (BMP) family**, and the **glial cell line-derived neurotrophic factor (GDNF)** family function as important pleiotropic modulators of nociceptive processing under physiologically and pathologically diverse painful conditions (Chen et al., 2013; Chen et al., 2016; Dong & He, 2014; Gardell et al., 2003; Malin et al., 2006; Merighi, 2016; Tramullas et al., 2010), suggesting that targeting specific members of the superfamily and their signalling pathways may provide beneficial effects on the mechanism and promising molecular targets for novel therapies in chronic neuropathic pain (Lantero et al., 2012; Lees et al., 2015; Merighi, 2016).

As a specific member of the activin and inhibin family, **activin C** is considered to be distinct from **activin A** and other activins in its subunit constitution, distribution pattern, and especially in its signalling pathway and functions (Marino, Risbridger, & Gold, 2015; Reader, Marino, Nicholson, Risbridger, & Gold, 2018). A previous study has reported that activin C is expressed in small dorsal root ganglion (DRG) neurons and is reportedly reduced in lumbar (L)4–5 DRGs in rats with chronic inflammatory pain, playing an antinociceptive role in inflammatory pain (Liu et al., 2012). However, the functions of activin C in neuropathic pain remain to be fully defined.

Accordingly, we performed sciatic nerve axotomy in rats to observe the expression of activin C mRNA and protein in L4–5 DRG neurons with a custom microarray, real-time RT-PCR, western

What is already known

- Activin C is expressed in small-diameter DRG neurons and functions to suppress inflammatory pain.

What this study adds

- Investigation of analgesic effects of activin C on neuropathic pain in peripheral nerve injury rodents.

What is the clinical significance

- This study identifies activin C as a new potential therapeutic for alleviating chronic neuropathic pain.

blotting, and immunofluorescence. We also performed behavioural tests in rodents to determine the therapeutic effects of activin C on chronic neuropathic pain following intrathecal and peripheral administration. We used whole-cell electrophysiological recordings, **capsaicin**-induced pain-related behaviour tests, and **TRPV1** channel knockout (KO) mice to investigate the mechanisms of activin C-induced analgesia. Our study provides robust evidence for the application of activin C in neuropathic pain therapy.

2 | METHODS

2.1 | Animals

All animal care and experimental procedures were carried out according to the guidelines of the International Association for the Study of Pain and approved by the Committee of Use of Laboratory Animals, Nantong University. Animal studies are reported in compliance with the ARRIVE guidelines (Percie du Sert et al., 2020) and with the recommendations made by the British Journal of Pharmacology (Lilley et al., 2020). To avoid the confounding effects of the oestrous cycle on pain processing, only male animals were used in this study.

Adult male (200–250 g) Sprague–Dawley (SD) rats, young male SD rats (90–110 g), and 8- to 12-week-old male C57/BL mice were provided by SLAC Laboratory Animal Company (Shanghai, China).

TRPV1 KO mice were purchased from Jackson Laboratory (Bar Harbor, ME, USA) and were crossed with adult female C57BL/6J wild-type (WT) mice. MaleTRPV1 KO and WT mice (8- to 12-week-old, housed in separate cages) of the same background were used for behavioural testing. Rats (two per cage) and mice (two to five per cage) were housed under standard conditions (21–24°C, 60% humidity, 12:12-h light/dark cycle), with free access to water and food.

2.2 | Sciatic nerve axotomy, autotomy score, and DRG isolation

To perform the sciatic nerve axotomy, adult rats were deeply anaesthetized with 3% pentobarbital sodium (80 mg·kg^{-1}). The left sciatic nerves were transected at the mid-thigh level, and nerves (1.0 cm) were removed from axotomized rats.

On days 0.5, 1, 2, 7, 14, and 28 after surgery and on day 0 as an intact control (n = 9 rats per time point), the experimental animals were anaesthetized and perfused, via the left ventricle, with cold 0.1-M PBS (pH 7.4) and the L4–5 DRGs were rapidly isolated under RNase free conditions.

For axotomy score, the levels of autotomy were scored daily for each rat for 4 weeks, as modified from a previous report in a double-blind manner (Xu et al., 2013). Briefly, 0.1 point was assigned to the loss of 1 nail or 1 bleeding finger, and 1 point was assigned for each distal half digit attacked. Then an additional point was added for each proximal half digit attacked. Rats reaching 10 points were killed humanely.

2.3 | Microarray and real-time RT-PCR

Microarray and quantitative RT-PCR were performed as described previously (Liu et al., 2012). Experimental rats were deeply anaesthetized with 3% pentobarbital sodium (80 mg·kg^{-1}), and then L4–5 DRGs were immediately dissected out. Total RNA was isolated from the isolated DRGs using the Agilent total RNA isolation mini kit and further used as a template for cDNA synthesis. Transcription was performed in vitro using an Agilent low RNA input fluorescent linear amplification kit in the presence of Cy3- and Cy5-CTP. Synthesized fluorescence-labelled cRNAs were used for the microarray. The hybridization solution was prepared according to the instructions of an Agilent hybridization kit plus, and hybridization was performed using the custom microarray at 60°C for 18 h with a dye-swap replication protocol. A microarray scanner system (Agilent Technologies, Inc.) was used for scanning and data analysis. After feature extraction with the Feature Extraction software, log2 ratios were calculated. Compared with the expression on day 0, genes whose expression exhibited a log2 ratio ≥1 (≥2-fold increase) were considered to be up-regulated, and those with log2 ratio ≤ −1 (≥2-fold decrease) were considered to be down-regulated. Following filtration and the normalization of each qualified gene, microarray data were visualized using Cluster 3.0 and TreeView software (Eisen Lab, Stanford, CA, USA).

Quantitative RT-PCR was performed on an ABI 7700 system (Applied Biosystems, Foster City, CA, USA). The SYBR PrimeScript RT-PCR Kit was used following the manufacturer's instructions. The expression of activin C (Inhbc) gene (NM_022614, forward primer 5′-TTTTGTGGCAGCCCAGGTAA-3′ and reverse primer 5′-AGCCAATCTC ACGGAAGTCCA-3′) and the control gene GAPDH (forward primer 5′-ATCACCATCTTCCAGGAGCGA-3′ and reverse primer 5′-AGCCTTCTCCATGGTGGTGAA-3′) were analysed. Activin C gene expression was normalized according to the expression level of GAPDH from the same sample. Changes in the expression of the activin C gene are presented as fold changes when compared with the day 0 control.

2.4 | Western blotting

Immunoblotting was performed according to a previous protocol (Liu et al., 2012). The antibody-based procedures used here comply with the recommendations made by the *British Journal of Pharmacology*. Experimental rats were deeply anaesthetized with 3% pentobarbital sodium (80 mg·kg^{-1}), and then L4–5 DRGs were isolated. DRG neurons were collected and lysed in RIPA buffer containing protease inhibitor cocktails (Sigma-Aldrich). Then the protein samples were loaded on denatured sodium dodecyl sulfate gels for electrophoresis and subsequently transferred to nitrocellulose membranes and incubated with antibodies against activin C (1:5,000; AbD Serotec, Kidlington, Oxford, UK) or GAPDH (1:10,000; Abcam, Cambridge, MA, USA) as an internal control overnight at 4°C. The target bands were detected by HRP-conjugated secondary antibodies and visualized with an ECL system. The bands of interest from films were quantified using Image-Pro Plus 6.0 (La Jolla, CA, USA). Then the intensity of the activin C-immunostaining band was normalized to the GAPDH intensity of the same sample.

2.5 | Immunohistochemistry staining

Immunofluorescence was performed as described in previous reports (Lin, Yu, Liu, et al., 2016; Lin, Yu, Wang, et al., 2016; Lin et al., 2017; Liu et al., 2016). Deeply anaesthetized rats (3% pentobarbital sodium, 80 mg·kg^{-1}) were perfused with 4% paraformaldehyde and 0.02% picric acid in PBS. L4–5 DRGs and spinal cords (SCs) were isolated and fixed in 4% paraformaldehyde for 1.5 h and overnight, respectively. DRG sections (14 μm for rat and 7 μm for mouse) and 14-μm SC sections were prepared using a cryostat. For activin C staining, antigen retrieval was performed with Frozen Section Chemical Antigen Retrieval Reagent, and sections were then permeabilized and blocked. For other immunostaining experiments, the antigen retrieval procedure was not necessary. The sections were incubated overnight at 4°C with a goat primary antibody against βC subunit (1:100; Santa Cruz Biotechnology, Santa Cruz, CA, USA), combined with a rabbit antibody against CGRP (1:2,000; AbD Serotec) and a guinea pig antibody against NeuN (1:2,000; Millipore, Billerica, MA, USA), or with

goat anti-IBA-1 (ionized calcium-binding adapter molecule 1; 1:300; Abcam) combined with mouse anti-GFAP (glial fibrillary acidic protein; 1:300; Cell Signaling Technology, Danvers, MA, USA). Next, the sections were incubated with secondary antibodies. Tile scanning of the fluorescence images was performed with an LSM 800 laser-scanning confocal imaging system (Carl Zeiss, AG, Jena, Germany), and Image-Pro Plus 6.0 was used to analyse the fluorescence signals. For quantification of the immunostaining results, at least three sections were selected from each animal, and three to six animals from each group were blindly analysed. To determine the percentage of labelled neurons in DRGs, the number of positive neurons (3 times of the background signal) was divided by the total number of neurons. For IBA-1 and GFAP immunostaining, the number of positive cells was counted, and/or the density of labelled cells (per square mm) was determined.

2.6 | Spinal nerve ligation model

Spinal nerve ligation (SNL) was performed as described previously (Jiang et al., 2016; Lu et al., 2014). After the experimental rats were anaesthetized using 3% **pentobarbital sodium** (50 mg·kg^{-1}), the L5–6 spinal nerves were ligated and cut, with the L4 spinal nerves left intact. On day 7 after SNL, the paw withdrawal threshold was determined using von Frey filaments. To assess its modulatory role in SNL rats, activin C was dissolved in 20 μl of PBS containing 0.2% BSA and then intrathecally injected in the experimental rats. The paw withdrawal threshold was measured at indicated time points.

2.7 | Chronic constriction injury model

Chronic constriction injury (CCI) was performed on adult mice as previously described (Liu et al., 2016; Xu et al., 2013). Under 1% pentobarbital sodium anaesthesia (65 mg·kg^{-1}), the mouse sciatic nerve was exposed, and three ligatures (6-0 Prolene) were applied around the nerve proximal to the trifurcation. The ligatures were loosely tied, and the distance between each ligature was 1 mm. The sham group underwent the same surgery without nerve ligation.

2.8 | Intrathecal injection

To investigate the antinociceptive effects of spinally applied activin C, the study compound was intrathecally administered as previously described (Joksimovic et al., 2020; Liu et al., 2012). After briefly anaesthetizing animals with **isoflurane** (2.5%), the dorsal surface of each animal was shaved to expose the injection site. The site for the subarachnoid puncture was determined by palpation at the iliac bone tuberosities, the spinous process of the last lumbar vertebra, and below the lumbosacral space. The L5–6 intervertebral spaces were identified by sliding the index finger along the midline in the rostral direction. A sterile 30-G needle approached the midline of the intervertebral space, with the bevel of the needle facing rostrally. When the needle tip reached the intervertebral space 2–3 mm in-depth, the precise subarachnoid positioning of the needle tip was verified by brisk tail-flicking. Then the reagent (20 μl) was injected into the subarachnoid space at the cauda equina region. The needle was left in the place for 5 s before withdrawing to avoid the reflux of the injected drug.

2.9 | Von Frey and Hargreaves tests

Both tests were carried out as described in previous reports (Liu et al., 2016; Xu et al., 2013). For mechanical pain measurement, the paw withdrawal threshold to von Frey filament stimulation was determined in rats and mice. Animals were placed in a box on an elevated metal mesh floor to habituate for 30 min, and their hind paws were stimulated with a series of von Frey hairs with logarithmically increasing stiffness (0.16, 0.40, 0.60, 1.00, and 2.00 g for mice; 2.00, 4.00, 800, 15.00, 26.00, and 60.00 g for rats; Ugo Basile, Gemonio, Varese, Italy). The hairs were applied perpendicular to the plantar surface of the paw, and the 50% paw withdrawal threshold was determined using Dixon's up-down method. After 30 min of acclimation, the paw withdrawal latency to radiant heat for thermal pain measurement was determined as the average of three or four measurements per paw over a 5-min period of testing with Hargreaves radiant heat apparatus (IITC, Woodland Hills, CA, USA). To prevent tissue injury, the light beam was automatically cut off at 20 s. To assess its modulatory role in CCI mice, activin C was dissolved in PBS containing 0.2% BSA and then locally pre-applied to the ligated sciatic nerves of CCI mice immediately after sciatic nerve ligation.

2.10 | Electrophysiology

Electrophysiological recordings were performed as described previously (Ma, Zhang, Dong, Bao, & Zhang, 2015; Yang et al., 2017). Young rats (90–110 g) were deeply anaesthetized with 3% pentobarbital sodium (80 mg·kg^{-1}), and then L4–5 DRGs were quickly excised. The DRGs were digested with trypsin type I and collagenase type 1A and then mechanically dissociated with Pasteur pipettes. The dissociated cells were placed on glass coverslips, and a patch-clamp recording was performed within 2 h to examine neuronal excitability. Neurons were considered TRPV1-positive if an inward current was observed after the application of capsaicin (1.0 μM). To explore the effect of activin C on capsaicin-induced TRPV1 channel currents, we exposed neurons to capsaicin after incubation with activin C (100 ng·ml^{-1}) or the vehicle. All data were collected with an EPC-9 patch-clamp amplifier. The MATLAB program was used to analyse action potential parameters. For assessing the desensitization of TRPV1 channels, the second or third capsaicin-induced current was normalized to the first capsaicin-induced current, as different neurons exhibit different amplitudes of TRPV1 channel currents after exposure to capsaicin.

2.11 | Haematoxylin and eosin staining

Deeply anaesthetized mice (2% pentobarbital sodium, 100 mg·kg^{-1}) were perfused with 4% paraformaldehyde and 0.02% picric acid in PBS. The sciatic nerves were removed, fixed in 4% paraformaldehyde overnight at 4°C, dehydrated, and then embedded in paraffin. Next, tissues were cut at a 5-μm thickness, fixed on glass slides, and baked to dryness. According to the instructions (H&E Staining Kit, Beijing Solarbio Science & Technology Co., Ltd, Beijing, China), the sections were soaked in xylene and gradient concentrations of ethanol and then stained using haematoxylin and eosin. The slides were rinsed, dehydrated, cleared, and then mounted with resin. Images were acquired using an optical microscope (Olympus DP22; Olympus, Tokyo, Japan).

2.12 | Intraplantar injection of capsaicin in mice

This test was performed as previously described (Nersesyan et al., 2017). Mice were handled and habituated and then intradermally injected with carrier-free rh-activin C (20 ng in 20 μl of PBS) or PBS (20 μl) as a vehicle control into hind paws, with a 26-G needle. After 15 min, the mice received an intraplantar injection of capsaicin (1.6 μg per paw in 20 μl of PBS containing 5% ethanol and 5% Tween 80) at the same site and were immediately returned to their chambers for video recording for 5 min. Finally, pain-related behaviour observed in the videos was quantified in a blind manner by counting the pain response time.

2.13 | Paw oedema measurement

For assessing mouse paw oedema, the average of three paw thickness measurements was recorded using a microcaliper after intraplantar capsaicin injection, at the indicated time points in a blind manner.

2.14 | Hot and cold plate tests

Both tests were performed with a hot/cold plate (Ugo Basile). Briefly, mice were individually placed on the plate for at least 20 min·day^{-1}, on 3 subsequent days for habituation before the behavioural tests. Then the cold plate test was performed at 4°C with a cut-off of 120 s, and the hot plate test was performed at 52°C with a cut-off of 60 s. The paw withdrawal latency was calculated as the mean value of three measurements with intervals of at least 5 min.

2.15 | Data and statistical analyses

The data and statistical analysis comply with the recommendations of the *British Journal of Pharmacology* on experimental design and analysis in pharmacology (Curtis et al., 2018). All data were collected with Microsoft Excel and further analysed using GraphPad Prism 6.0 (La Jolla, CA, USA). Statistical analysis was undertaken only for studies where each group size was $n \geq 5$. The declared animal or sample sizes were the number of independent values, and statistical analyses were performed using these independent values. For all axotomy experiments, rats were randomly used. However, for behavioural pain experiments, to control unwanted variations in the pain threshold before and after modelling and ensure the comparability of pain thresholds at multiple time points before and after drug treatment, litter-matched and age-matched animals were assigned to experimental groups to generate biological replicates based on their baselines and pre-administration values (pain threshold), and behavioural tests and data analyses were performed in a blinded manner. All behavioural experiments were performed in a quiet room and evaluated by blinded investigators. For all experiments, no outliers were excluded. To control the unwanted variations of sources and backgrounds, normalization of the data was conducted and is expressed as fold of control. All western blotting and immunohistochemical procedures and analysis comply with the recommendations detailed in the *BJP* editorial (Alexander et al., 2018). All data sets were tested for normality and equal variance and then were analysed using the Student's unpaired *t*-test (for two groups), one-way repeated-measures ANOVA (for multiple groups), or two-way repeated-measures ANOVA followed by post hoc Bonferroni multiple comparisons test (for time course comparison) using GraphPad Prism 6.0. All data are expressed as the mean ± SEM and were considered statistically significant at a *P*-value of <0.05.

2.16 | Materials

Recombinant human (rh)-activin C was purchased from R&D Systems (Minneapolis, MN, USA). Total RNA isolation mini kit was purchased from Agilent Technologies Inc. (Santa Clara, CA, USA). The SYBR PrimeScript RT-PCR Kit was provided by Takara Biotechnology Co., Ltd. (Dalian, LN, China). Paraformaldehyde, picric acid, trypsin type I, collagenase type 1A, DNase I, pentobarbital sodium, BSA, protease inhibitor cocktails, and capsaicin were purchased from Sigma-Aldrich (St. Louis, MO, USA). Enhanced ECL system was purchased from Roche Diagnostics GmbH (Roche Diagnostics, Mannheim, Germany). DMEM was provided by Gibco-Invitrogen (Carlsbad, CA, USA). Frozen Section Chemical Antigen Retrieval Reagent was provided by GenMed Scientifics (Wilmington, DE, USA). RIPA buffer and protease inhibitor cocktail were provided by Thermo Fisher Scientific Inc. (Rockford, IL, USA).

2.17 | Nomenclature of targets and ligands

Key protein targets and ligands in this article are hyperlinked to corresponding entries in http://www.guidetopharmacology.org, and are permanently archived in the Concise Guide to PHARMACOLOGY 2019/20 (Alexander et al., 2019).

3 | RESULTS

3.1 | Up-regulation of activin C in lumbar DRGs of peripheral nerve-injured rats

To determine the dose of activin C to be intrathecally injected in adult rats, we first investigated the expression of this cytokine in the lumbar DRGs of rats with chronic neuropathic pain. We performed sciatic nerve axotomy in rats, a simple and feasible model of peripheral nerve injury. Employing a custom microarray (Liu et al., 2012), we observed a robust up-regulation of activin βC mRNA in the L4–5 DRGs of rats after axotomy, when compared with L4–5 DRGs of control rats on day 0 (Figure 1a). We further confirmed the change in activin βC mRNA expression by real-time RT-PCR and observed that the expression of activin βC mRNA tended to increase after axotomy (Figure 1b). Then we performed western blotting to observe the expression of activin C protein and found that the expression of activin C (a 25-kDa band indicating two βC subunits) increased after axotomy (Figure 1c,d), suggesting that there were similar increasing trends in the expression of activin C protein (βCβC) and activin βC subunit mRNA.

Next, we performed immunofluorescence to determine the cellular localization of activin C and observed that activin C was mainly expressed in small-diameter neurons (Figure 2a), consistent with a previous report (Liu et al., 2012). As expected, quantification analysis showed that the percentage of activin C-positive neurons was robustly increased (3,882 of 8,607 total neurons from nine rats) in L4–5 DRGs of axotomized rats on day 14, compared with sham control rats (1,691 of 5,634 total neurons from nine rats), consistent with the microarray, real-time RT-PCR and western blot data (Figure 1). However, in the peptidergic subset, CGRP-positive neurons were significantly decreased on day 14 after axotomy (2,209 of 8,607 total neurons from nine rats), compared with sham control rats (2,461 of 5,634 total neurons from nine rats; Figure 2a,b), which is consistent with the nerve injury condition. Accordingly, all axotomized rats developed different degrees of autotomy, a pain-related behaviour accompanied with axotomy, within 4 weeks (n = 9 rats), whereas the sham rats did not exhibit any autotomy (n = 7 rats; Figure 2c). In the CCI mouse model, activin C-positive neurons also increased, while CGRP-positive neurons decreased, in L4–5 DRGs of CCI mice on day 7 by immunofluorescence (Figure 2e). Hence, we concluded that activin C was markedly up-regulated in L4–5 DRGs, following peripheral nerve injury.
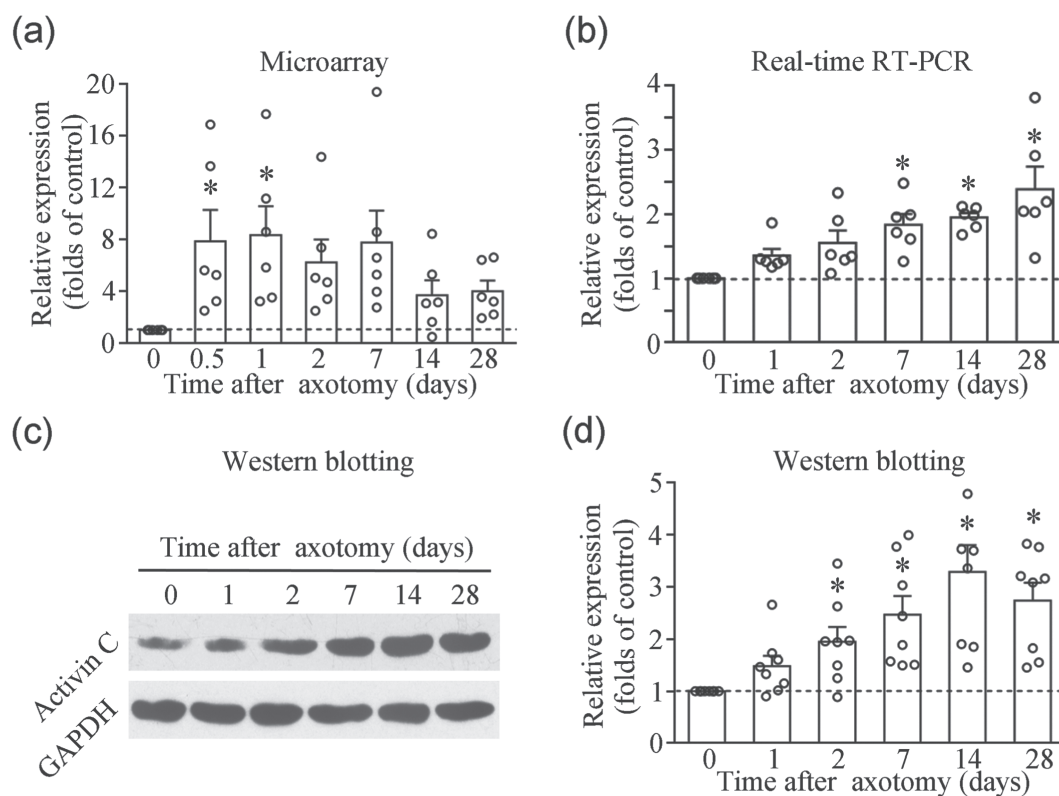

FIGURE 1   Up-regulation of activin βC subunit mRNA and activin C protein expression in the lumbar (L)4–5 dorsal root ganglia (DRGs) of rats following sciatic nerve axotomy. (a) Custom microarray result. n = 6 separate experiments. (b) Real-time RT-PCR analysis. n = 6 separate experiments. (c) Immunoblotting at 25 kDa demonstrates activin C consisting of βCβC subunits, as shown by western blotting. (d) Quantitative analysis of eight independent western blotting experiments showing the up-regulation of activin C protein in the L4–5 DRGs of axotomized rats. DRG from n = 9–12 rats per time point. Data are presented as mean ± SEM. *P < 0.05, significantly different from day 0 (naïve) control rats; one-way repeated-measures ANOVA followed by post hoc Bonferroni multiple comparisons test
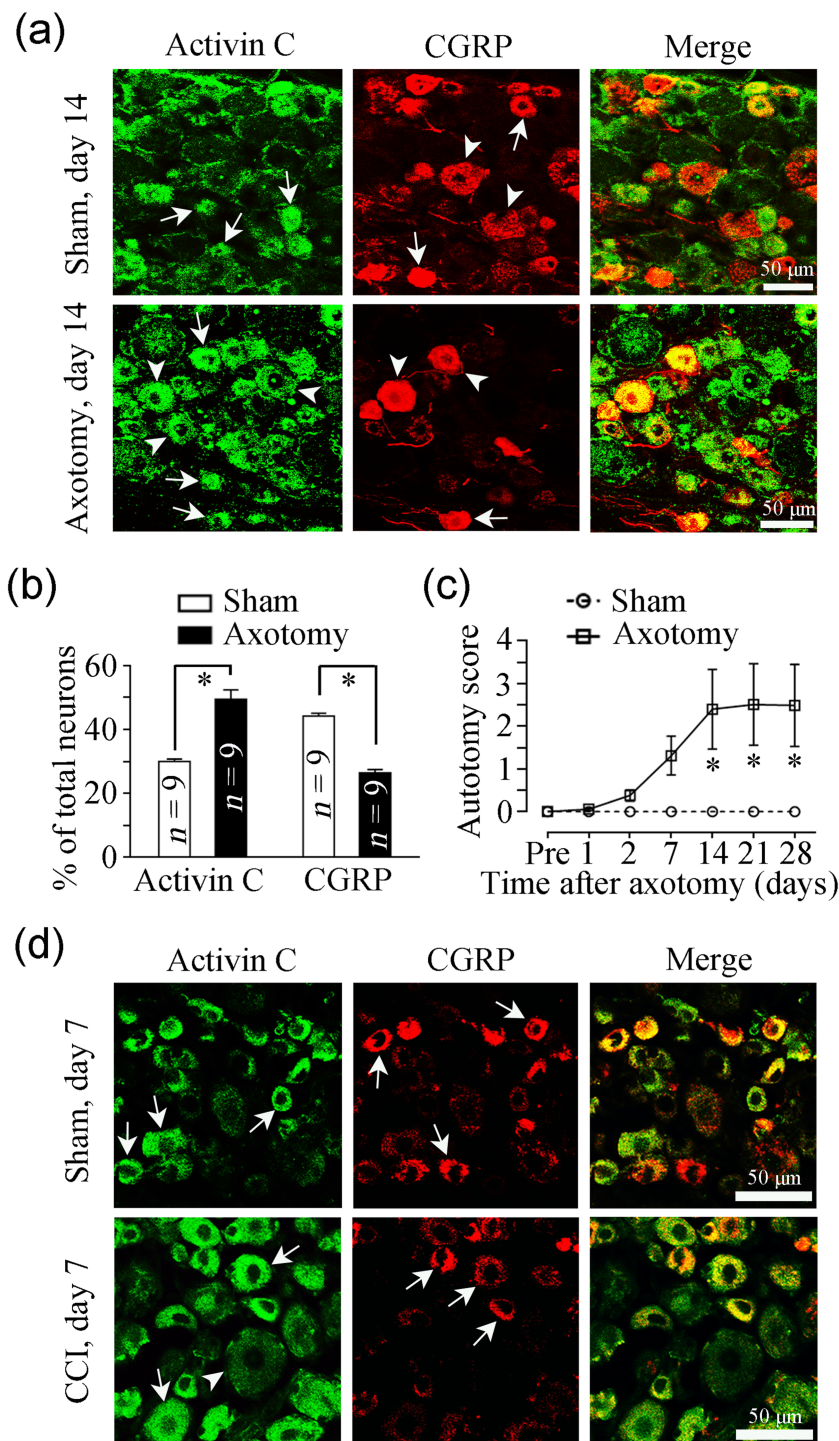
FIGURE 2 Up-regulation of activin C protein expression in the lumbar (L)4–5 dorsal root ganglia (DRGs) of peripheral nerve injury rodents observed by double-immunofluorescence staining. (a) Activin C protein-positive small-diameter neurons and co-expression of activin C with CGRP in the L4–5 DRG of sham control rats increase activin C protein-positive small-diameter neurons and decrease co-expression of activin C with CGRP in the L4–5 DRG of axotomized rats on day 14 after axotomy. (b) Quantitative analysis of the immunofluorescence results showing the percentage of activin C-positive neurons and CGRP-positive neurons in the L4–5 DRGs of naïve and axotomized rats on day 14 after axotomy. (c) The degree of autotomy (self-mutilation) in axotomized and sham rats within 4 weeks. (d) Double-immunofluorescence staining indicates an increase in activin C-positive small- and medium-diameter neurons and a decrease in the co-expression of activin C with CGRP in the L4–5 DRGs of CCI mice on day 7 after CCI. Arrows indicate the small-diameter neurons (≤30 μm in diameter); arrowheads indicate the medium-diameter neurons (30–45 μm). Data are presented as mean ± SEM. *$P < 0.05$, significantly different from sham animals; one-way repeated-measures ANOVA followed by post hoc Bonferroni multiple comparisons test

3.2 | Intrathecal or peripheral administration of activin C suppresses chronic neuropathic pain

In a previous study, activin C was reportedly decreased in L4–5 DRGs and dose-dependently (50, 100, and 200 ng) inhibited chronic inflammatory pain, induced by complete Freund's adjuvant in rats (Liu et al., 2012). Based on the up-regulation of activin C expression after nerve injury (Figure 1), we first employed a high dose of 200 ng of activin C to investigate its effects in chronic neuropathic pain in a rat SNL model. After mechanical pain thresholds were significantly decreased on day 7 after SNL (Figure 3a left), the rats received a single intrathecal administration of 200 ng of rh-activin C or vehicle (20 μl). Unexpectedly, a single treatment with 200 ng of rh-activin C almost restored the mechanical hyperalgesia to baseline levels in SNL rats when applied for 2 h (Figure 3a right). We then used decreasing doses of 200, 100, and 50 ng and the same model to further investigate the dose-dependent analgesic effects of activin C. Intrathecal administration of 50, 100, or 200 ng of rh-activin C dose-dependently

FIGURE 3 Antinociceptive effects of activin C in spinal nerve ligation (SNL) rats and chronic constriction injury (CCI) mice. (a) Mechanical pain sensitivity develops on day 7 after SNL (left), and a single intrathecal injection of recombinant human (rh)-activin C (200 ng in 20 μl of PBS) increases the paw withdrawal threshold in rats that underwent SNL (right). (b) In SNL rats, mechanical pain sensitivity develops on day 7 after SNL (left), and a single intrathecal injection of 50,100, or 200 ng of rh-activin C dose-dependently increases the paw withdrawal threshold (right). (c, d) The long-term antinociceptive effect of local preincubation with 250 ng of activin C (in 200 μl of PBS) on thermal pain (c) and mechanic pain (d) in CCI mice. (e) Mechanical pain sensitivity develops on day 7 after CCI (left), and a single intrathecal injection of rh-activin C (15 ng in 5 μl of PBS) increases the paw withdrawal threshold in CCI mice (right). BS, baseline; PWL, paw withdrawal latency; PWT, paw withdrawal threshold. Data are presented as mean ± SEM. *$P < 0.05$, significantly different from baseline or vehicle control; two-way repeated-measures ANOVA followed by post hoc Bonferroni multiple comparisons test
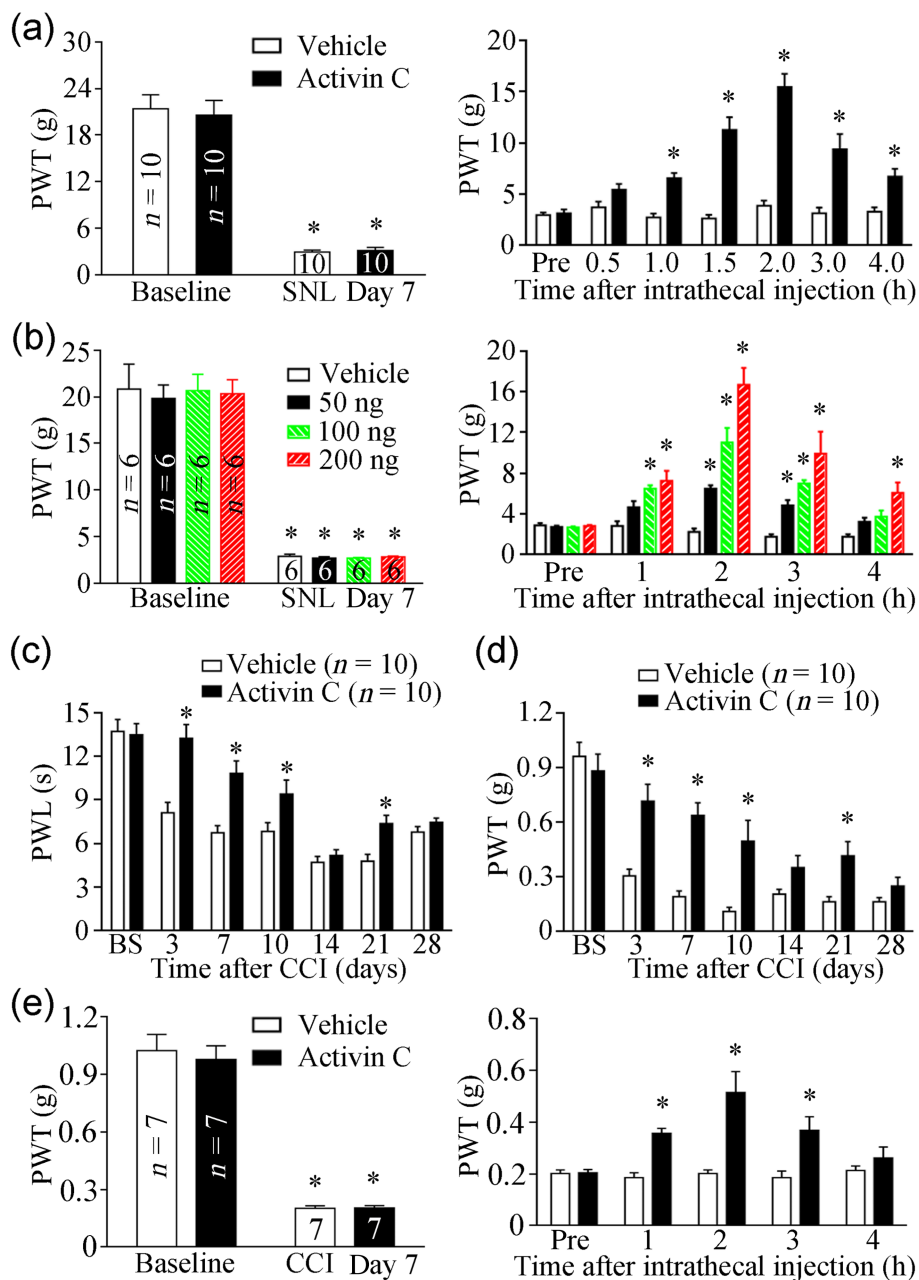
ameliorated chronic neuropathic pain, with a peak effect at 2 h post-injection (Figure 3b right).

The TGF-β superfamily is one of the most evolutionarily conserved signal transduction pathways within *Drosophila, C. elegans*, and vertebrates, especially within mammals sharing highly conserved components of the superfamily (Akhurst & Padgett, 2015). Considering the evolutionary conservation of the TGF-β superfamily and highly reduced dose of activin C in mice, we further investigated the peripheral effects of activin C on CCI-induced chronic neuropathic pain in mice, locally pretreated with 250 ng of rh-activin C. Compared with vehicle treatment, the immediate local pre-exposure of the ligated sciatic nerves to rh-activin C (in 200 μl of PBS) after sciatic nerve ligation not only attenuated thermal hyperalgesia (Figure 3c) but also inhibited mechanical hyperalgesia induced by CCI (Figure 3d). Notably, as shown in Figure 3c, local pretreatment with activin C postponed the onset of thermal pain from day 3 to day 7, suggesting that pre-administration of activin C impaired the development and the maintenance of thermal hyperalgesia induced by peripheral nerve injury. To further assess the effect of activin C on established pain evoked by CCI, another group of CCI mice was investigated. After mechanical pain thresholds significantly decreased by day 7 of CCI (Figure 3e left), mice were intrathecally administered a single dose of 15 ng of rh-activin C or vehicle (5 μl). Mice treated with activin C exhibited significantly reduced mechanical hyperalgesia when compared with vehicle-treated mice (Figure 3e right).

3.3 | Pre-administration of activin C alleviates CCI-evoked inflammatory responses in the nervous system but not at local injury sites

Inflammatory cell (macrophage) infiltration into DRGs and activation of glial cells (microglia and astrocytes) in the SC have been implicated in the genesis of neuropathic pain (Calvo, Dawes, & Bennett, 2012; Liu et al., 2016; Xu et al., 2013). We employed immunofluorescence to examine cellular changes in inflammatory responses in the L4–5 DRGs and spinal dorsal horns (SDHs) on day 7 following CCI. As shown in

Figures 4 and 5, sciatic nerve injury induced by CCI elicited significant macrophage infiltration into the ipsilateral DRGs and a robust microglial reaction in the ipsilateral SDHs (both indicated by increased IBA-1 immunoreactivity), and both these effects were blocked by local pretreatment with activin C, but not with the vehicle (11–24 sections from six mice; Figures 4a,b and 5a,b). Satellite cell reactions in DRGs and astrocyte reactions in SDHs (both indicated by increased GFAP immunoreactivity) were not significantly increased on the ipsilateral side when compared with the contralateral side at day 7 after CCI (11–24 sections from six mice; Figures 4a,c and 5a,c). However, the
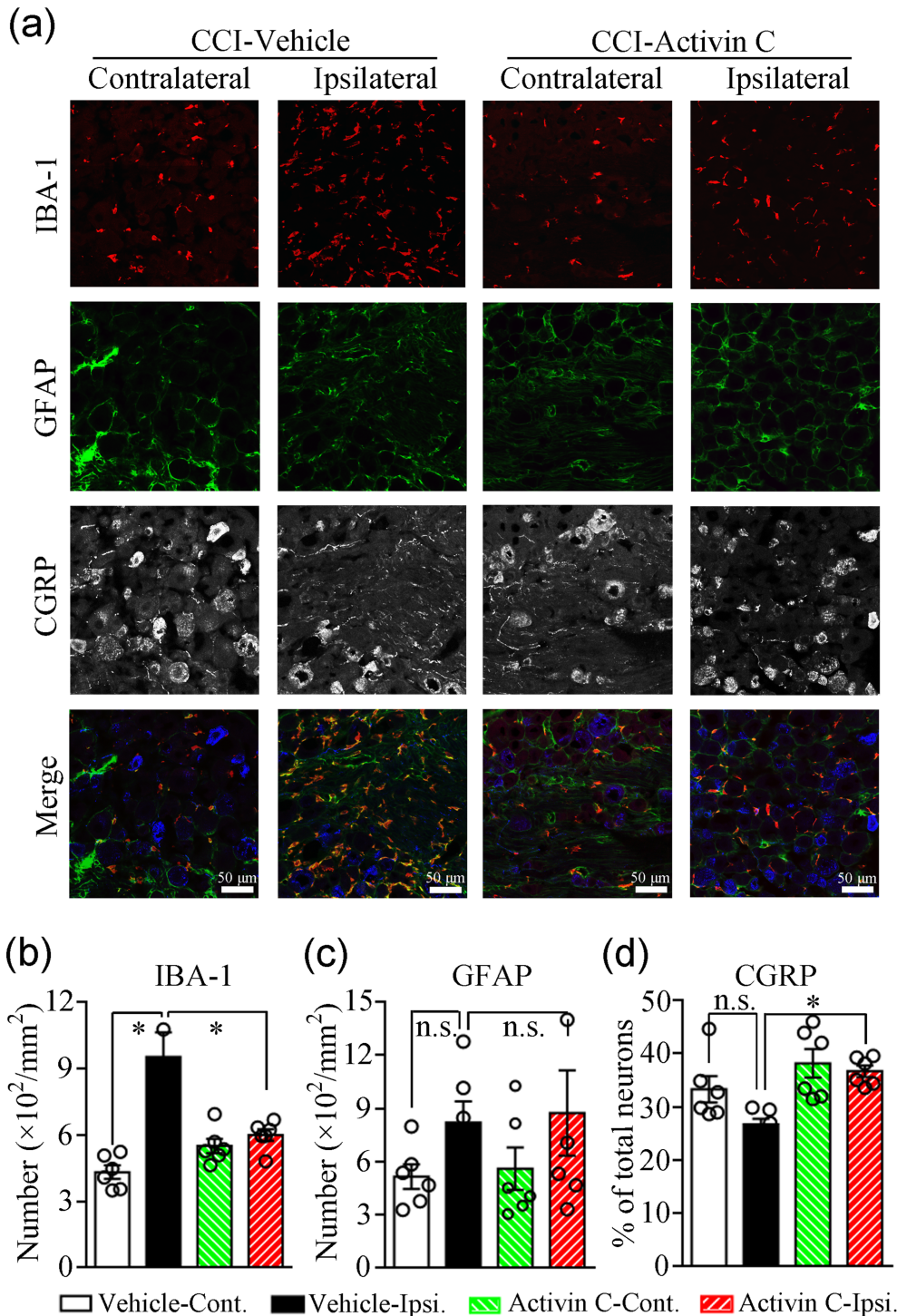

FIGURE 4 Triple immunofluorescence labelling for IBA-1, GFAP, and CGRP in the lumbar 4–5 dorsal root ganglia (DRGs) of chronic constriction injury (CCI) mice pretreated with activin C (250 ng in 200 μl of PBS) or PBS (200 μl) on day 7 after CCI. (a) Immunofluorescence images. CGRP immunofluorescence was set to blue in the merged images. (b–d) Quantitative analysis of the number of IBA-1-positive macrophages (b), the number of GFAP-positive satellite cells (c), and the percentage of CGRP-positive neurons (d) by immunofluorescence. n = 6 mice; n.s., no significance; Cont., contralateral; Ipsi., ipsilateral; IBA-1, ionized calcium-binding adaptor molecule 1 (Iba1); GFAP, glial fibrillary acidic protein (GFAP). Data are presented as mean ± SEM. *$P < 0.05$, significantly different as indicated; one-way repeated-measures ANOVA followed by post hoc Bonferroni multiple comparisons test

FIGURE 5 Triple immunofluorescence labelling for IBA-1, GFAP, and CGRP in the lumbar 4–5 spinal dorsal horns (SDHs) of chronic constriction injury (CCI) mice pre-administered activin C (250 ng in 200 μl of PBS) or PBS (200 μl) on day 7 after CCI. (a) Immunofluorescence images. (b–d) Quantitative analysis for the number of IBA-1-positive microglia (b), the density of GFAP immunoreactivity (c), and the density ratio of CGRP immunoreactivity (d). $n = 6$ mice; Cont., contralateral; Ipsi., ipsilateral; IBA-1, ionized calcium-binding adaptor molecule 1 (Iba1); GFAP, glial fibrillary acidic protein (GFAP). Data are presented as mean ± SEM. *$P < 0.05$, significantly different as indicated; one-way repeated-measures ANOVA followed by post hoc Bonferroni multiple comparisons test for (b) and (c) and unpaired two-tailed t-test with Welch's correction for (d)
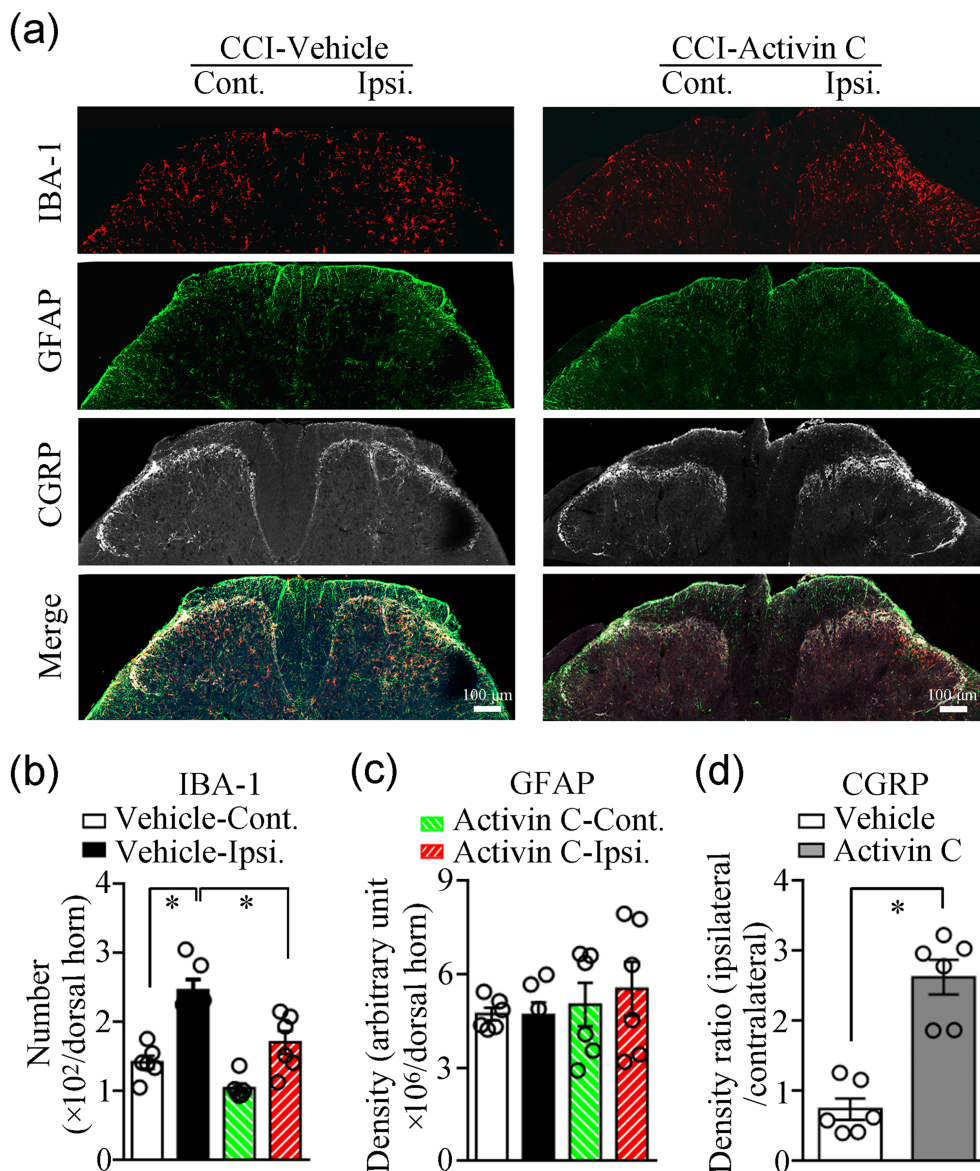
number of satellite cells exhibited an increasing trend in the DRGs of CCI mice. Furthermore, local pretreatment with activin C did not exhibit an obvious effect on satellite cells and astrocytes (11–24 sections from six mice; Figures 4c and 5c). In contrast, we aimed to determine local inflammatory responses in ligated sciatic nerves after local pretreatment with activin C by measuring tissue swelling and inflammatory cell infiltration. Local pre-administration of activin C did not affect local nerve oedema (Figure 6a,b) or inflammatory cell infiltration (Figure 6c) induced by CCI in local ligated sciatic nerves.

3.4 | Peripheral pre-treatment with activin C normalizes CGRP expression in DRGs and SDHs in CCI mice

Largely produced by peptidergic neurons in DRGs and transported to central and peripheral nerves, CGRP is an important peptide for the modulation of pain perception (de Vries & MaassenVanDenBrink, 2019;

Nees et al., 2016), although its function in neuropathic pain remains controversial (Iyengar, Ossipov, & Johnson, 2017). In the present study, CGRP expression exhibited a decreasing trend in the injured DRGs and SDHs (11–24 sections from six mice; Figures 4a,d and 5a,d). Interestingly, local pretreatment with activin C reversed CGRP down-regulation in the ipsilateral DRGs (Figure 4a,d) and SDHs (Figure 5a,d) on day 7 after CCI, suggesting that the pretreatment with activin C normalized CGRP expression in DRGs and SDHs and the normalization of CGRP expression might benefit the analgesic effects of activin C.

3.5 | Activin C enhances capsaicin-induced currents in lumbar DRG neurons of rats

To further explore the possible mechanisms of antinociceptive functions of activin C underlying chronic neuropathic pain, we acutely dissociated single L4–5 DRG neurons from naïve young rats and performed whole-cell electrophysiological recordings on small-diameter
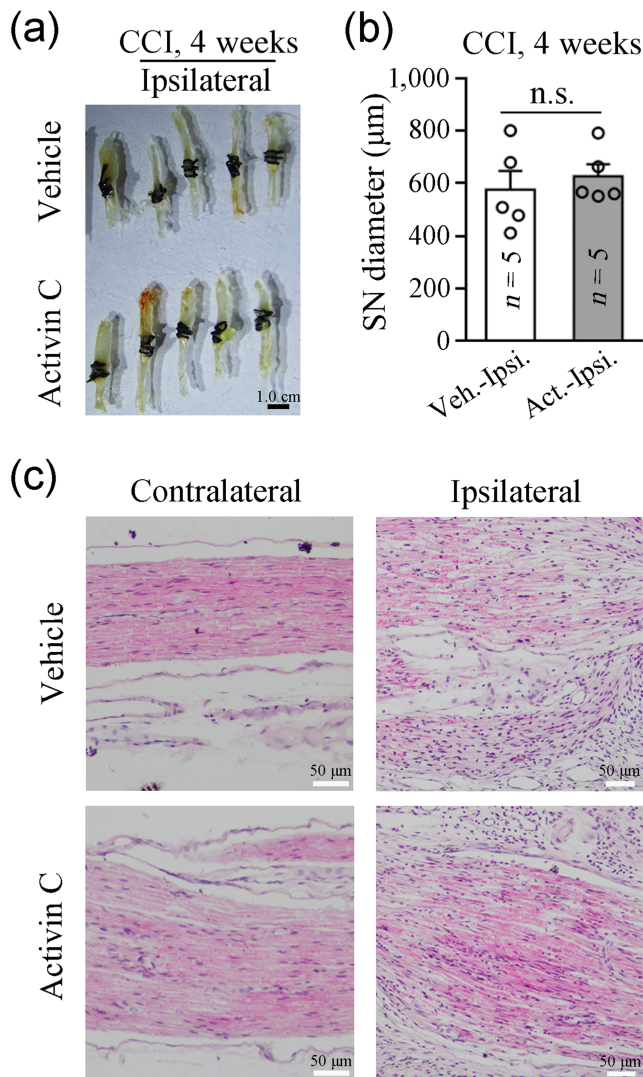
FIGURE 6 Peripheral pretreatment with activin C does not affect chronic constriction injury (CCI)-evoked inflammatory responses in local ligated sciatic nerves. (a) Images of ligated sciatic nerves on day 28 after CCI excised from CCI mice pre-administered activin C (250 ng in 200 μl of PBS) or vehicle (200 μl of PBS). (b) Quantitative analysis of local oedema in the exercised ligated sciatic nerves shown in (a) was performed by measuring the sciatic nerve diameter from pictures using the Image-Pro Plus 6.0 software. SN, sciatic nerve; Veh., vehicle; Cont., contralateral; Act., activin C; Ipsi., ipsilateral. (c) Haematoxylin and eosin staining shows no difference in the inflammatory cell infiltration in local ligated nerves between pretreated with activin C and those pretreated with vehicle on day 7 after CCI. Data are presented as mean ± SEM. n.s., non-significant; one-way repeated-measures ANOVA followed by post hoc Bonferroni multiple comparisons test

FIGURE 7 Activin C enhances capsaicin-induced TRPV1 channel currents in rat dorsal root ganglia (DRG) neurons. (a) A whole-cell recording showing the desensitization of TRPV1 currents by three successive exposures to capsaicin (1.0 μM). (b) A whole-cell recording showing that preincubation with activin C (100 ng·ml^{-1}) enhances the TRPV1 currents provoked by successive capsaicin incubations. (c) Quantitative analysis of (a) and (b). n = 6 mice for the vehicle or 7 mice for activin C; Cap, capsaicin; ECS, extracellular solution. Data are presented as mean ± SEM, *P < 0.05, significantly different from vehicle; one-way repeated-measures ANOVA followed by post hoc Bonferroni multiple comparisons test

desensitization phenotype in second and third TRPV1 currents evoked by capsaicin (7–11 neurons from six to seven mice; Figure 7a,c). We suggested that activin C may regulate TRPV1 channel current by accelerating TRPV1 channel desensitization to relieve neuropathic pain.

3.6 | Activin C reduces capsaicin-evoked acute hyperalgesia and normalizes lasting hypothermia in mice

Based on the above electrophysiological data, we postulated that activin C modulates the function of TRPV1 channels to attenuate

neurons. We observed that activin C (100 ng·ml^{-1}) failed to evoke any current by itself (data not shown). However, preincubation of capsaicin-responsive small-diameter neurons with activin C (100 ng·ml^{-1}) for 5 or 10 min significantly enhanced the amplitudes of capsaicin-induced TRPV1 currents (7–11 neurons from six to seven mice; Figure 7b,c) when compared with those observed after preincubation with the extracellular solution (ECS) that induced a
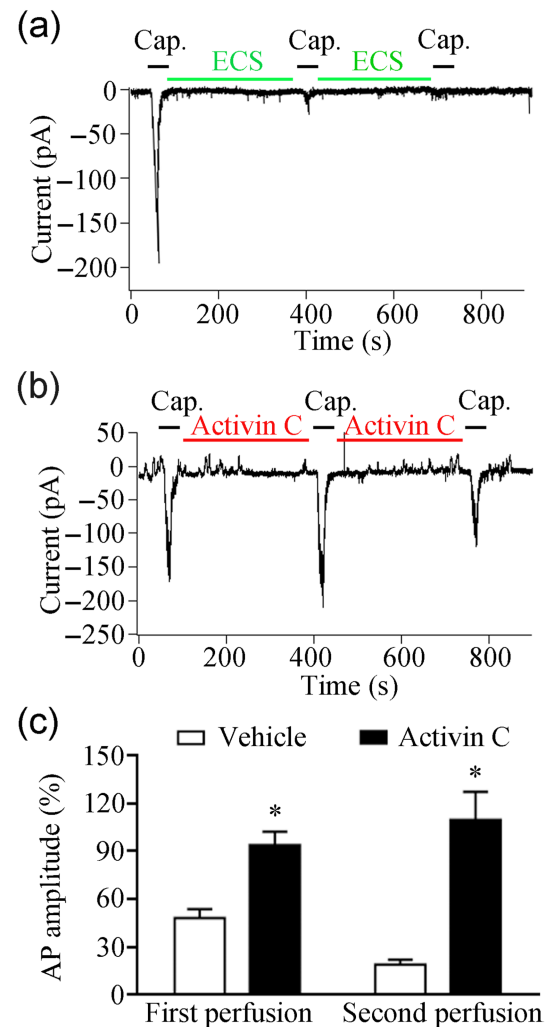
chronic neuropathic pain (Nersesyan et al., 2017). To further test this hypothesis, we performed behavioural experiments measuring capsaicin-induced pain-related behaviour to quantify acute nocifensive and long-lasting temperature insensitivity in mice after the local intraplantar injection of vehicle/activin C and capsaicin. Local intraplantar application of activin C (20 ng in 20 μl of PBS per paw) alone did not provoke any noticeable aversive responses in mice (data not shown), consistent with a previous finding observed in rats (Liu et al., 2012). However, compared with pre-injection of the vehicle, pretreatment with activin C (20 ng) significantly inhibited acute nocifensive behaviour evoked by the capsaicin injection (Figure 8a). Then we evaluated local tissue swelling by measuring the paw diameter. Notably, pretreatment with activin C did not affect paw oedema induced by the capsaicin injection (Figure 8b), suggesting that activin C does not affect local neurogenic inflammation. Next, we further observed the long-lasting temperature insensitivity behaviours using hot and cold plate tests and found that activin C normalized persistent

hypoalgesia to heat and cold stimuli induced by a single intraplantar injection of capsaicin (Figure 8c,d).

3.7 | TRPV1 channels are essential for analgesic effects of activin C in chronic neuropathic pain

To further validate the hypothesis that TRPV1 channels are an analgesic target of activin C in vivo, we investigated the antinociceptive function of activin C in CCI-induced chronic neuropathic pain in WT mice and TRPV1 KO mice. Activin C or the vehicle was pre-applied as described earlier in the CCI model, and then the mechanical hyperalgesia in these mice was monitored in response to mechanical stimuli during the next 4 weeks. As shown in Figure 8e, CCI mice (including WT and TRPV1 KO) exhibited significant mechanical hyperalgesia when compared with sham control mice. Although TRPV1 KO mice exhibited higher mechanical pain thresholds, local
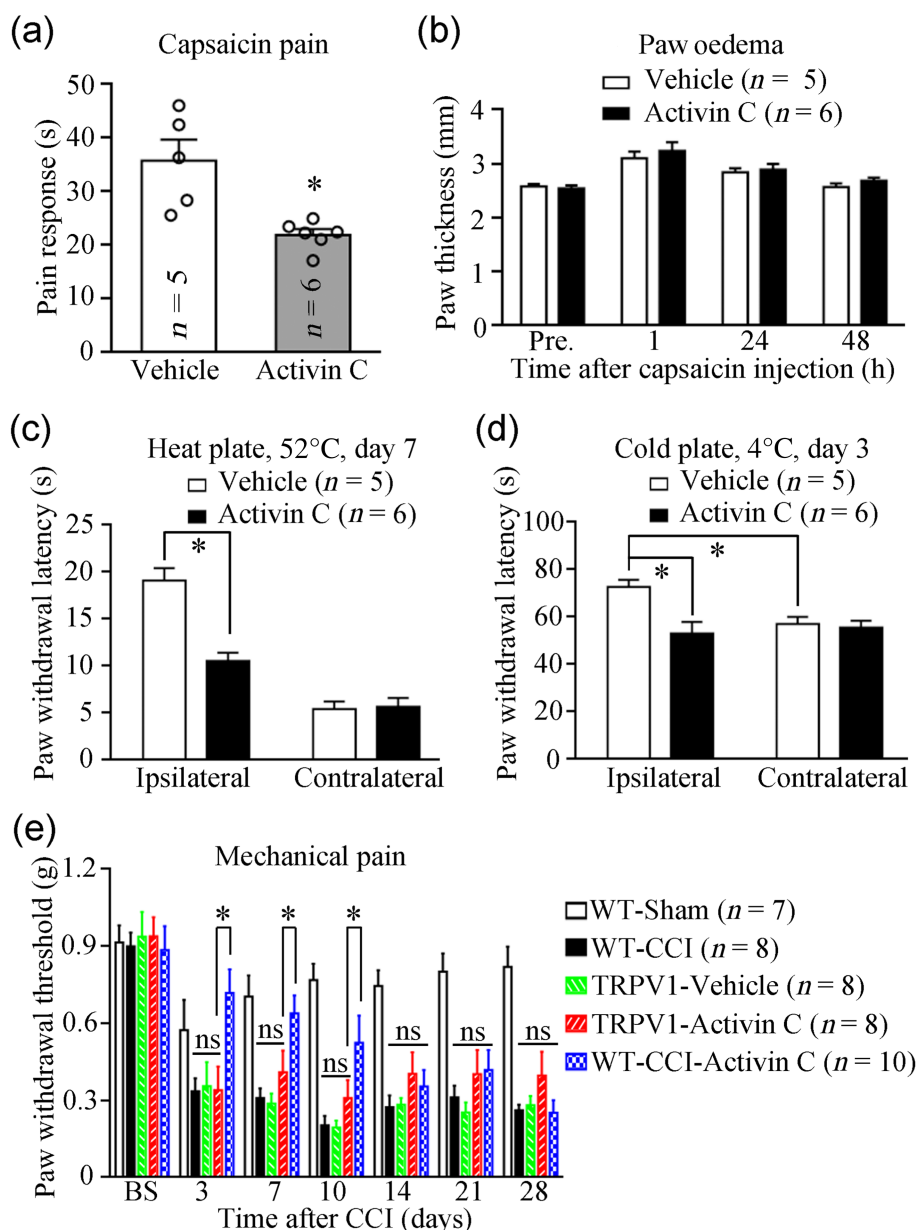

FIGURE 8 Further confirmation of TRPV1 channel modulation by activin C using behavioural tests in mice. (a) Activin C (20 ng in 20 μl of PBS, pre-intraplantar injection) ameliorates acute nocifensive behaviour induced by intraplantar injection of capsaicin. (b) Paw oedema evoked by capsaicin injection. (c, d) Activin C (20 ng in 20 μl of PBS, pre-intraplantar injection) normalized long-lasting heat hypothermia (52°C) on day 7 (c) and cold hypothermia (4°C) on day 3 (d) after capsaicin injection. (e) The analgesic effects of activin C (250 ng in 200 μl of PBS, preincubation) on neuropathic pain induced by chronic constriction injury are abolished in TRPV1 KO mice. Pre, pre-administration. Data are presented as mean ± SEM. ns, no significant difference; *$P < 0.05$, significantly different from vehicle for (a), significantly different as indicated for (c), (d) and (e); unpaired two-tailed t-test for (a), one-way repeated-measures ANOVA followed by post hoc Bonferroni multiple comparisons test for (c) and (d), and two-way repeated-measures ANOVA followed by post hoc Bonferroni multiple comparisons test for (e)

pretreatment with activin C (250 ng in 200 μl of PBS) did not signifi-
cantly alter mechanical hyperalgesia in TRPV1 KO CCI mice, when
compared with the vehicle control and WT CCI mice (Figure 8e).

4 | DISCUSSION

In this study, we demonstrated that activin C exerts analgesic effects
in chronic neuropathic pain following both intrathecal and peripheral
administration, which represent common routes of analgesic applica-
tions in clinical practice. We employed multiple approaches and three
neuropathic pain models to determine the effects of activin C on neu-
ropathic pain. Our study supports a relationship between the antino-
ciception mediated via activin C and modulation of TRPV1 channel
activity, suggesting that activin C may be a potential candidate for
neuropathic pain therapy. However, our conclusion is based on animal
experiments performed with solely in males, and these findings may
not apply to females.

As neuropathic pain has multiple aetiologies, we used axotomy,
SNL, and CCI models to assess the effects of activin C on neuropathic
pain. The axotomy model is reliable and easily reproducible and clini-
cally simulates phantom limb pain. Furthermore, more DRGs can be
acquired for screening genes. The SNL model is suitable for studying
injured and uninjured nerve fibres in the sciatic nerve and mimics the
symptoms of human patients suffering from causalgia, developed after
peripheral nerve injury and sympathetic nerve-mediated pain. The CCI
model involves both neuropathic and inflammatory components and
mimics causalgia, post-traumatic peripheral painful neuropathy,
entrapment neuropathy, and complex regional pain syndrome in
patients. Furthermore, following peripheral nerve injury, immune cells
of DRGs and SCs release cytokines to sensitize/desensitize nocicep-
tive neurons and further modulate pain processing (de Miguel,
Kraychete, & Meyer Nascimento, 2014; Ebersberger, 2018; Lees
et al., 2015). Importantly, some primary sensory neurons were found
to also secrete cytokines that directly regulate nociceptive processing
(Chen et al., 2013; Liu et al., 2012; Nersesyan et al., 2017; Thakur
et al., 2017). Moreover, robust evidence suggests that targeting the
TGF-β superfamily signalling has beneficial effects in chronic neuro-
pathic pain (Dong & He, 2014; Ebersberger, 2018; Lantero
et al., 2012; Tramullas et al., 2010). Thus, we hypothesized that addi-
tional components of the TGF-β superfamily might be involved in pain
processing and act as potential targets for neuropathic pain treatment.
In this study, we used a custom microarray to screen significant
changes in mRNA levels of TGF-β superfamily members in L4–5 DRGs
of axotomized rats, compared with naïve control rats. We found that
activin βC gene expression was up-regulated in axotomized DRGs.
Next, we further confirmed the transcriptional increase in the activin
βC subunit by real-time RT-PCR, as well as the increased expression
of activin C protein by western blotting and immunofluorescence.
Furthermore, increased expression of activin C was confirmed in the
CCI mouse model. These data indicate that activin C is up-regulated
at both the mRNA and protein levels in lumbar DRGs after peripheral
nerve injury. Consistently, the up-regulation of activin C was

correlated with the degree of autotomy, a pain-related self-mutilation
behaviour, in axotomized rats and with mechanical and thermal
hyperalgesia in CCI mice, strongly suggesting a role for activin C in
neuropathic pain.

To further clarify the central and peripheral effects of activin C
in neuropathic pain, we adopted two models, SNL in rats and CCI in
mice. Based on the up-regulation of activin C after nerve injury, we
first selected a high dose of activin C (200 ng) to investigate its
effects on neuropathic pain in a rat SNL model and found that the
intrathecal administration of 200 ng of activin C almost reversed
the mechanical hyperalgesia, to approximately baseline values. Then
we employed a range of doses of activin C to confirm the analgesic
effects of activin C and observed that the intrathecal administration
of 50, 100, or 200 ng of rh-activin C dose-dependently inhibited
neuropathic pain in SNL rats. Considering that tissues around
injured nerves absorb a large amount of activin C injected locally,
we selected a high (250 ng) to ensure that the injured nerves were
able to absorb an adequate amount. The antinociceptive effect of
activin C was observed in CCI mice following mechanical and ther-
mal stimulation by locally pre-administering activin C to ligated sci-
atic nerves. Moreover, a single intrathecal administration of activin
C inhibited the established mechanical pain in CCI mice. These data
indicate that the central or peripheral administration of activin C
relieves chronic neuropathic pain in rats and mice, similar to other
TGF-β superfamily members (Chen et al., 2013; Chen et al., 2016;
Lantero et al., 2012; Lees et al., 2015; Malin et al., 2006; Tramullas
et al., 2010).

Inflammatory cell infiltration into the DRGs and activation of glial
cells in the SCs have been implicated in the genesis of neuropathic
pain (Calvo et al., 2012; Liu et al., 2016; Xu et al., 2013). Consistent
with this concept, local pretreatment with activin C inhibited macro-
phage infiltration into lumbar DRGs and the proliferation of activated
microglia in the SCs, while local treatment with activin C did not affect
satellite cells or astrocytes in the early phase of CCI. Furthermore,
local pre-administration of activin C did not affect nerve oedema or
inflammatory responses in local ligated nerves. These results indicate
that peripheral pretreatment with activin C prevents CCI-evoked
inflammatory responses in the peripheral nervous system and CNS
but not in local neurogenic inflammation. Hence, we postulated that
pretreatment with exogenous activin C inhibits nociceptive signal
transmission from the peripheral nerves to the innervated DRGs and
SCs and further reduced CCI-evoked inflammatory responses in DRGs
and SCs (Sommer, Leinders, & Uceyler, 2018), but not through a direct
anti-inflammatory mechanism. Although activin A plays a role in the
early phase of inflammatory processes (Dong & He, 2014) and is a
critical component of the inflammatory response (Jones et al., 2007),
our data did not support the idea that activin C may antagonize activin
A-induced hyperalgesia (Dong & He, 2014). One possibility is that
activin C, like TGF-β1, acts as an analgesic by suppressing
neuroimmune responses of neurons and glia, decreasing the activity
of spinal excitatory neurons, and inhibiting some pain signalling path-
ways (Chen et al., 2013; Chen et al., 2016; Lantero et al., 2012; Lees
et al., 2015).

However, local pretreatment with activin C did not have an obvious effect on the activation or proliferation of astrocytes, and we postulate that the effects of activin C on astrocyte activation during the late phase of CCI should be further investigated. Unexpectedly, local pre-administration of activin C normalized the reduced CGRP levels induced by CCI in the ipsilateral DRGs and SCs, suggesting that the cytokine, activin C, has multiple actions in the nervous system and may regulate the release of diverse pain-related neurotransmitters, including CGRP, after peripheral nerve injury. Similarly, activin A was found to synergistically regulate CGRP expression with nerve growth factor in vitro (Xu & Hall, 2007), but activin C and activin A exhibit completely distinct actions in pain processing. Notably, all Aβ-fibres and a majority of the Aδ-fibres are axotomized, whereas a large number of C-fibres remain intact in the CCI model (all fibres are axotomized in the axotomy model and partial Aβ-, Aδ-, and C-fibres are axotomized in the SNL model). Hence, CCI-evoked pain is possibly mediated by C- and/or A-δ fibres, including the majority of CGRP[+] fibres. Concerning the unexpected functions of CGRP (Baral et al., 2018; Wallrapp et al., 2019; Xu et al., 2019), the crosstalk between activin C and CGRP warrants further investigation.

Considering that TRPV1 channels are non-selective Ca^{2+} channels expressed mainly in the cell bodies of sensory neurons and conveys pain signal under sensitization (Moore, Gupta, Jordt, Chen, & Liedtke, 2018; Moran & Szallasi, 2018; Patapoutian, Tate, & Woolf, 2009), we postulate that activin C might directly or indirectly engage in crosstalk with TRPV1 channels in DRG neurons to modulate neuropathic pain (Nersesyan et al., 2017). Our electrophysiological analysis showed that although activin C alone demonstrated no effect on TRPV1 currents in single dissociated DRG neurons, pre-incubation with activin C significantly increased capsaicin-induced TRPV1 currents. Considering that capsaicin is a specific TRPV1 agonist that quickly opens TRPV1 channels to induce pain sensation in the short term (Chung & Campbell, 2016) and that pretreatment with activin C requires a long period to enhance capsaicin-induced TRPV1 currents, we hypothesized that enhancing TRPV1 channel activity by activin C is an indirect pathway, which differs from that of activin A which acutely sensitized the capsaicin-induced current (Zhu, Xu, Cuascut, Hall, & Oxford, 2007). However, persistent stimulation by capsaicin elicits TRPV1 desensitization and renders the channels unable to reopen in the long term, which in turn disrupts pain signal transmission in DRG neurons and their afferents (Chung & Campbell, 2016; Nersesyan et al., 2017). The mechanism by which activin C modulates TRPV1 channels was further confirmed by nocifensive mouse behaviour; activin C attenuated the capsaicin-induced acute nociceptive response. This is consistent with the use of capsaicin as the main component of painkillers in clinical practice (Ghouri & Conaghan, 2019). However, pretreatment with activin C did not reduce the mouse paw oedema evoked by the capsaicin injection, suggesting that the antinocifensive function of activin C is not achieved by reducing local oedema or inflammation. Interestingly, activin C pretreatment normalized the capsaicin-induced lasting hypothermia following heat and cold stimuli in mice. Taking the normalized CGRP data together, it is possible that activin C has complex functions in the nervous system, which warrant further evaluation. As expected, the analgesic effects of activin C were abolished in TRPV1 KO mice after CCI. These data provide solid evidence that activin C ameliorates chronic neuropathic pain by modulating TRPV1 channel function, facilitating our understanding that exogenous activin C promotes the release of CGRP, as TRPV1 channels mediate secretion of CGRP and substance P in DRG neurons. Although TRPV1 KO mice exhibited intact mechanical hyperalgesia in this CCI model, a recent study showed that when the TRPV1 gene in adult rodents was knocked down by siRNA, the CCI-induced behavioural hyperalgesia was reduced (Guo et al., 2019). This discrepancy suggests that genetic compensation should be commonplace in the TRPs family. However, the several unknown functions of activin C, including its specific receptor, need to be further investigated.

In conclusion, the present study demonstrated that endogenous activin C is predominantly expressed and markedly up-regulated in small DRG neurons after peripheral nerve injury and that activin C, given by either peripheral or intrathecal application suppressed chronic neuropathic pain by modulating TRPV1 channels, suggesting that activin C may have therapeutic potential for the treatment of chronic neuropathic pain.

ACKNOWLEDGEMENTS

AUTHOR CONTRIBUTIONS

X.J.L. designed experiments and analysed the data; X.J.L. and Y.G.L. wrote the main draft of the manuscript; X.J.L., X.Z., and Y.G.L. performed the custom microarray and real-time PCR. Y.K.H., X.Z., F.M.Z., Y.C., and Q.Y.L. performed behavioural tests and analysed the data; J.B.Z., J.H.G., L.B.B., Z.J.J., X.M.W., and Y.L. performed western blot and immunofluorescence and analysed the data; Y.K.H., X.M.W., and J.X.S. performed the electrophysiological test and analysed the data; Y.K.H., J.B.Z., and Y.L. performed H&E staining. X.J.L. supervised the whole study. All authors approved the final version of the manuscript.

CONFLICT OF INTERESTS

The authors declare no competing interests.

DECLARATION OF TRANSPARENCY AND SCIENTIFIC RIGOUR

This Declaration acknowledges that this paper adheres to the principles for transparent reporting and scientific rigour of preclinical research as stated in the *BJP* guidelines for Design & Analysis, Immunoblotting and Immunochemistry, and Animal Experimentation, and as recommended by funding agencies, publishers, and other organizations engaged with supporting research.

DATA AVAILABILITY STATEMENT

The data that support the findings of this study are available from the corresponding author upon reasonable request. Some data may not be made available because of privacy or ethical restrictions.

ORCID

Xing-Jun Liu https://orcid.org/0000-0002-5496-541X

REFERENCES

Agarwal, N., Helmstadter, J., Rojas, D. R., Bali, K. K., Gangadharan, V., & Kuner, R. (2018). Evoked hypoalgesia is accompanied by tonic pain and immune cell infiltration in the dorsal root ganglia at late stages of diabetic neuropathy in mice. *Molecular Pain*, 14, 1744806918817975. https://doi.org/10.1177/1744806918817975

Akhurst, R. J., & Padgett, R. W. (2015). Matters of context guide future research in TGFβ superfamily signaling. *Science Signaling*, 8(399), re10. https://doi.org/10.1126/scisignal.aad0416

Alexander, S. P. H., Mathie, A., Peters, J. A., Veale, E. L., Striessnig, J., Kelly, E., ... CGTP Collaborators. (2019). The Concise Guide to PHARMACOLOGY 2019/20: Ion channels. *British Journal of Pharmacology*, 176, S142–S228. https://doi.org/10.1111/bph.14749

Alexander, S. P. H., Roberts, R. E., Broughton, B. R. S., Sobey, C. G., George, C. H., Stanford, S. C., ... Ahluwalia, A. (2018). Goals and practicalities of immunoblotting and immunohistochemistry: A guide for submission to the *British Journal of Pharmacology*. *British Journal of Pharmacology*, 175, 407–411. https://doi.org/10.1111/bph.14112

Baral, P., Udit, S., & Chiu, I. M. (2019). Pain and immunity: Implications for host defence. *Nature Reviews. Immunology*, 19, 433–447. https://doi.org/10.1038/s41577-019-0147-2

Baral, P., Umans, B. D., Li, L., Wallrapp, A., Bist, M., Kirschbaum, T., ... Chiu, I. M. (2018). Nociceptor sensory neurons suppress neutrophil and γδ T cell responses in bacterial lung infections and lethal pneumonia. *Nature Medicine*, 24, 417–426. https://doi.org/10.1038/nm.4501

Calvo, M., Dawes, J. M., & Bennett, D. L. (2012). The role of the immune system in the generation of neuropathic pain. *Lancet Neurology*, 11, 629–642. https://doi.org/10.1016/S1474-4422(12)70134-5

Chen, N. F., Chen, W. F., Sung, C. S., Lu, C. H., Chen, C. L., Hung, H. C., ... Huang, S. Y. (2016). Contributions of p38 and ERK to the antinociceptive effects of TGF-β1 in chronic constriction injury-induced neuropathic rats. *The Journal of Headache and Pain*, 17, 72. https://doi.org/10.1186/s10194-016-0665-2

Chen, N. F., Huang, S. Y., Chen, W. F., Chen, C. H., Lu, C. H., Chen, C. L., ... Wen, Z. H. (2013). TGF-β1 attenuates spinal neuroinflammation and the excitatory amino acid system in rats with neuropathic pain. *The Journal of Pain*, 14, 1671–1685. https://doi.org/10.1016/j.jpain.2013.08.010

Chung, M. K., & Campbell, J. N. (2016). Use of capsaicin to treat pain: Mechanistic and therapeutic considerations. *Pharmaceuticals*, 9, 66. https://doi.org/10.3390/ph9040066

Curtis, M. J., Alexander, S., Cirino, G., Docherty, J. R., George, C. H., Giembycz, M. A., ... Ahluwalia, A. (2018). Experimental design and analysis and their reporting II: Updated and simplified guidance for authors and peer reviewers. *Brit J Pharmacol*, 175, 987–993. https://doi.org/10.1111/bph.14153

Dong, F., & He, X. (2014). Activin A: A potential therapeutic target for characterizing and stopping joint pain early in rheumatoid arthritis patients. *Inflammation*, 37, 170–176. https://doi.org/10.1007/s10753-013-9727-7

Ebersberger, A. (2018). The analgesic potential of cytokine neutralization with biologicals. *European Journal of Pharmacology*, 835, 19–30. https://doi.org/10.1016/j.ejphar.2018.07.040

Gardell, L. R., Wang, R., Ehrenfels, C., Ossipov, M. H., Rossomando, A. J., Miller, S., ... Porreca, F. (2003). Multiple actions of systemic artemin in experimental neuropathy. *Nature Medicine*, 9, 1383–1389. https://doi.org/10.1038/nm944

Ghouri, A., & Conaghan, P. G. (2019). Treating osteoarthritis pain: Recent approaches using pharmacological therapies. *Clinical and Experimental Rheumatology*, 37, 124–129.

Guo, S. H., Lin, J. P., Huang, L. E., Yang, Y., Chen, C. Q., Li, N. N., ... Yao, Y. X. (2019). Silencing of spinal Trpv1 attenuates neuropathic pain in rats by inhibiting CAMKII expression and ERK2 phosphorylation. *Scientific Reports-UK*, 9(1), 2769. https://doi.org/10.1038/s41598-019-39184-4

Huang, T., Lin, S. H., Malewicz, N. M., Zhang, Y., Zhang, Y., Goulding, M., ... Ma, Q. (2019). Identifying the pathways required for coping behaviours associated with sustained pain. *Nature*, 565, 86–90. https://doi.org/10.1038/s41586-018-0793-8

Hung, A. L., Lim, M., & Doshi, T. L. (2017). Targeting cytokines for treatment of neuropathic pain. *Scandinavian Journal of Pain*, 17, 287–293. https://doi.org/10.1016/j.sjpain.2017.08.002

Iyengar, S., Ossipov, M. H., & Johnson, K. W. (2017). The role of calcitonin gene-related peptide in peripheral and central pain mechanisms including migraine. *Pain*, 158, 543–559. https://doi.org/10.1097/j.pain.0000000000000831

Ji, R. R. (2018). Recent progress in understanding the mechanisms of pain and itch: The second special issue. *Neuroscience Bulletin*, 34, 1–3. https://doi.org/10.1007/s12264-018-0204-z

Jiang, B. C., Cao, D. L., Zhang, X., Zhang, Z. J., He, L. N., Li, C. H., ... Gao, Y. J. (2016). CXCL13 drives spinal astrocyte activation and neuropathic pain via CXCR5. *The Journal of Clinical Investigation*, 126, 745–761. https://doi.org/10.1172/JCI81950

Joksimovic, S. L., Joksimovic, S. M., Manzella, F. M., Asnake, B., Orestes, P., Raol, Y. H., ... Todorovic, S. M. (2020). Novel neuroactive steroid with hypnotic and T-type calcium channel blocking properties exerts effective analgesia in a rodent model of post-surgical pain. *British Journal of Pharmacology*, 177, 1735–1753. https://doi.org/10.1111/bph.14930

Jones, K. L., Mansell, A., Patella, S., Scott, B. J., Hedger, M. P., de Kretser, D. M., & Phillips, D. J. (2007). Activin A is a critical component of the inflammatory response, and its binding protein, follistatin, reduces mortality in endotoxemia. *Proceedings of the National Academy of Sciences*, 104, 16239–16244. https://doi.org/10.1073/pnas.0705971104

Kuner, R. (2010). Central mechanisms of pathological pain. *Nature Medicine*, 16, 1258–1266. https://doi.org/10.1038/nm.2231

Lantero, A., Tramullas, M., Diaz, A., & Hurle, M. A. (2012). Transforming growth factor-β in normal nociceptive processing and pathological pain models. *Molecular Neurobiology*, 45, 76–86. https://doi.org/10.1007/s12035-011-8221-1

Lees, J. G., Fivelman, B., Duffy, S. S., Makker, P. G., Perera, C. J., & Moalem-Taylor, G. (2015). Cytokines in neuropathic pain and associated depression. *Mod Trends Pharmacopsychiatry*, 30, 51–66. https://doi.org/10.1159/000435932

Lin, S. F., Wang, B., Zhang, F. M., Fei, Y. H., Gu, J. H., Li, J., ... Liu, X. J. (2017). T-type calcium channels, but not Cav3.2, in the peripheral sensory afferents are involved in acute itch in mice. *Biochemical and Biophysical Research Communications*, 487, 801–806. https://doi.org/10.1016/j.bbrc.2017.04.127

Lin, S. F., Yu, X. L., Liu, X. Y., Wang, B., Li, C. H., Sun, Y. G., & Liu, X. J. (2016). Expression patterns of T-type Ca$_v$3.2 channel and insulin-like growth factor-1 receptor in dorsal root ganglion neurons of mice after sciatic nerve axotomy. *Neuroreport*, 27, 1174–1181. https://doi.org/10.1097/WNR.0000000000000676

Lin, S. F., Yu, X. L., Wang, B., Zhang, Y. J., Sun, Y. G., & Liu, X. J. (2016). Colocalization of insulin-like growth factor-1 receptor and T type Ca$_v$3.2 channel in dorsal root ganglia in chronic inflammatory pain

mouse model. *Neuroreport*, *27*, 737–743. https://doi.org/10.1097/WNR.0000000000000607

Liu, X. J., Liu, T., Chen, G., Wang, B., Yu, X. L., Yin, C., & Ji, R. R. (2016). TLR signaling adaptor protein MyD88 in primary sensory neurons contributes to persistent inflammatory and neuropathic pain and neuroinflammation. *Scientific Reports*, *6*, 28188. https://doi.org/10.1038/srep28188

Liu, X. J., Zhang, F. X., Liu, H., Li, K. C., Lu, Y. J., Wu, Q. F., ... Zhang, X. (2012). Activin C expressed in nociceptive afferent neurons is required for suppressing inflammatory pain. *Brain*, *135*, 391–403. https://doi.org/10.1093/brain/awr350

Lu, Y., Jiang, B. C., Cao, D. L., Zhang, Z. J., Zhang, X., Ji, R. R., & Gao, Y. J. (2014). TRAF6 upregulation in spinal astrocytes maintains neuropathic pain by integrating TNF-α and IL-1β signaling. *Pain*, *155*, 2618–2629. https://doi.org/10.1016/j.pain.2014.09.027

Ma, X. L., Zhang, F. X., Dong, F., Bao, L., & Zhang, X. (2015). Experimental evidence for alleviating nociceptive hypersensitivity by single application of capsaicin. *Molecular Pain*, *11*, 22. https://doi.org/10.1186/s12990-015-0019-0

Malin, S. A., Molliver, D. C., Koerber, H. R., Cornuet, P., Frye, R., Albers, K. M., & Davis, B. M. (2006). Glial cell line-derived neurotrophic factor family members sensitize nociceptors in vitro and produce thermal hyperalgesia in vivo. *The Journal of Neuroscience*, *26*, 8588–8599. https://doi.org/10.1523/JNEUROSCI.1726-06.2006

Marino, F. E., Risbridger, G., & Gold, E. (2015). Re-evaluating the role of activin-βC in cancer biology. *Cytokine & Growth Factor Reviews*, *26*, 463–470. https://doi.org/10.1016/j.cytogfr.2015.05.003

Merighi, A. (2016). Targeting the glial-derived neurotrophic factor and related molecules for controlling normal and pathologic pain. *Expert Opinion on Therapeutic Targets*, *20*, 193–208. https://doi.org/10.1517/14728222.2016.1085972

de Miguel, M., Kraychete, D. C., & Meyer Nascimento, R. J. (2014). Chronic pain: Cytokines, lymphocytes and chemokines. *Inflammation & Allergy Drug Targets*, *13*, 339–349. https://doi.org/10.2174/1871528114666150114170004

Moore, C., Gupta, R., Jordt, S. E., Chen, Y., & Liedtke, W. B. (2018). Regulation of pain and itch by TRP channels. *Neuroscience Bulletin*, *34*, 120–142. https://doi.org/10.1007/s12264-017-0200-8

Moran, M. M., & Szallasi, A. (2018). Targeting nociceptive transient receptor potential channels to treat chronic pain: Current state of the field. *Brit J Pharmacol*, *175*, 2185–2203. https://doi.org/10.1111/bph.14044

Nees, T. A., Tappe-Theodor, A., Sliwinski, C., Motsch, M., Rupp, R., Kuner, R., ... Blesch, A. (2016). Early-onset treadmill training reduces mechanical allodynia and modulates calcitonin gene-related peptide fiber density in lamina III/IV in a mouse model of spinal cord contusion injury. *Pain*, *157*, 687–697. https://doi.org/10.1097/j.pain.0000000000000422

Nersesyan, Y., Demirkhanyan, L., Cabezas-Bratesco, D., Oakes, V., Kusuda, R., Dawson, T., ... Zakharian, E. (2017). Oxytocin modulates nociception as an agonist of pain-sensing TRPV1. *Cell Reports*, *21*, 1681–1691. https://doi.org/10.1016/j.celrep.2017.10.063

Obara, I., Telezhkin, V., Alrashdi, I., & Chazot, P. L. (2020). Histamine, histamine receptors, and neuropathic pain relief. *British Journal of Pharmacology*, *177*, 580–599. https://doi.org/10.1111/bph.14696

Patapoutian, A., Tate, S., & Woolf, C. J. (2009). Transient receptor potential channels: Targeting pain at the source. *Nature Reviews. Drug Discovery*, *8*, 55–68. https://doi.org/10.1038/nrd2757

Percie du Sert, N., & Rice, A. S. (2014). Improving the translation of analgesic drugs to the clinic: Animal models of neuropathic pain. *British Journal of Pharmacology*, *171*, 2951–2963. https://doi.org/10.1111/bph.12645

Reader, K. L., Marino, F. E., Nicholson, H. D., Risbridger, G. P., & Gold, E. J. (2018). Role of activin C in normal ovaries and granulosa cell tumours of mice and humans. *Reproduction, Fertility, and Development*, *30*, 958–968. https://doi.org/10.1071/RD17250

Sommer, C., Leinders, M., & Uceyler, N. (2018). Inflammation in the pathophysiology of neuropathic pain. *Pain*, *159*, 595–602. https://doi.org/10.1097/j.pain.0000000000001122

Sun, S., Xu, Q., Guo, C., Guan, Y., Liu, Q., & Dong, X. (2017). Leaky gate model: Intensity-dependent coding of pain and itch in the spinal cord. *Neuron*, *93*(840–853), e845. https://doi.org/10.1016/j.neuron.2017.01.012

Thakur, K. K., Saini, J., Mahajan, K., Singh, D., Jayswal, D. P., Mishra, S., ... Kunnumakkara, A. B. (2017). Therapeutic implications of toll-like receptors in peripheral neuropathic pain. *Pharmacological Research*, *115*, 224–232. https://doi.org/10.1016/j.phrs.2016.11.019

Tramullas, M., Lantero, A., Diaz, A., Morchon, N., Merino, D., Villar, A., ... Hurle, M. A. (2010). BAMBI (bone morphogenetic protein and activin membrane-bound inhibitor) reveals the involvement of the transforming growth factor-β family in pain modulation. *The Journal of Neuroscience*, *30*, 1502–1511. https://doi.org/10.1523/JNEUROSCI.2584-09.2010

de Vries, T., & MaassenVanDenBrink, A. (2019). CGRP-targeted antibodies in difficult-to-treat migraine. *Nature Reviews. Neurology*, *15*, 688–689. https://doi.org/10.1038/s41582-019-0275-0

Wallrapp, A., Burkett, P. R., Riesenfeld, S. J., Kim, S. J., Christian, E., Abdulnour, R. E. E., ... Kuchroo, V. K. (2019). Calcitonin gene-related peptide negatively regulates alarmin-driven type 2 innate lymphoid cell responses. *Immunity*, *51*, 709–723.e6. https://doi.org/10.1016/j.immuni.2019.09.005

Xu, H. P., Ding, J. R., Porter, C. B. M., Wallrapp, A., Tabaka, M., Ma, S., ... Xavier, R. J. (2019). Transcriptional atlas of intestinal immune cells reveals that neuropeptide α-CGRP modulates group 2 innate lymphoid cell responses. *Immunity*, *51*, 696–708.e9. https://doi.org/10.1016/j.immuni.2019.09.004

Xu, P., & Hall, A. K. (2007). Activin acts with nerve growth factor to regulate calcitonin gene-related peptide mRNA in sensory neurons. *Neuroscience*, *150*, 665–674. https://doi.org/10.1016/j.neuroscience.2007.09.041

Xu, Z. Z., Liu, X. J., Berta, T., Park, C. K., Lu, N., Serhan, C. N., & Ji, R. R. (2013). Neuroprotectin/protectin D1 protects against neuropathic pain in mice after nerve trauma. *Annals of Neurology*, *74*, 490–495. https://doi.org/10.1002/ana.23928

Yang, L., Dong, F., Yang, Q., Yang, P. F., Wu, R., Wu, Q. F., ... Zhang, X. (2017). FGF13 selectively regulates heat nociception by interacting with Nav1.7. *Neuron*, *93*, 806–821 e809. https://doi.org/10.1016/j.neuron.2017.01.009

Zhu, W., Xu, P., Cuascut, F. X., Hall, A. K., & Oxford, G. S. (2007). Activin acutely sensitizes dorsal root ganglion neurons and induces hyperalgesia via PKC-mediated potentiation of transient receptor potential vanilloid I. *The Journal of Neuroscience*, *27*, 13770–13780. https://doi.org/10.1523/JNEUROSCI.3822-07.2007